JPSS-2 VIIRS Polarization Sensitivity Performance Comparison with Heritage VIIRS Sensors

D. Moyer[a], J. McIntire[b], H. Oudrari[b] and F. De Luccia[a]

[a]The Aerospace Corporation, 2310 El Segundo Blvd., El Segundo, CA 90245, [b]Science Systems and Applications, Inc., Lanham, MD 20706, USA2

ABSTRACT

The Joint Polar Satellite System 2 (JPSS-2) is the follow-on for the Suomi-National Polar-orbiting Partnership (S-NPP) and Joint Polar Satellite System 1 (JPSS-1) missions. These spacecrafts provide critical weather and global climate products to the user community. A primary sensor on both JPSS and S-NPP is the Visible-Infrared Imaging Radiometer Suite (VIIRS) with Earth observations covering the Reflective Solar Band (RSB), Thermal Emissive Band (TEB) and Day Night Band (DNB) spectral regions. The VIIRS Sensor Data Records (SDRs) contain the calibrated Earth observations that are used in Environmental Data Record (EDR) products such as Ocean Color/Chlorophyll (OCC) and Sea Surface Temperature (SST). This SDR calibration is performed using unpolarized sources such as the Solar Diffuser (SD) for the RSBs and an On-Board Calibrator BlackBody (OBCBB) for the TEBs. Therefore, polarized Earth scenes will have radiometric bias errors within the SDRs based on how sensitive VIIRS is to polarized illumination and is corrected in some EDR algorithms. This paper will discuss the JPSS-2 VIIRS polarization characterization methodology, polarization sensitivity results and compare its performance to its predecessors S-NPP and JPSS-1 VIIRS. Optical modifications to the JPSS-2 VIIRS sensor to address heritage polarization sensitivity issues will be discussed.

Keywords: Polarization, VIIRS, JPSS, S-NPP, Calibration

1. INTRODUCTION

The Visible Infrared Imaging Radiometer Suite (VIIRS) aboard the Suomi National Polar-orbiting Partnership (S-NPP), Joint Polar Satellite System 1 (JPSS-1) and JPSS-2 spacecrafts with launch dates of October 2011, November 2017 and ~2022 respectively, is a cross-track scanning sensor in a low Earth orbit [1]. Like its heritage sensors Operational Linescan System (OLS) [2], Moderate Resolution Imaging Spectroradiometer (MODIS) [3], and Advanced Very High Resolution Radiometer (AVHRR) [4], VIIRS provides calibrated top-of-atmosphere (TOA) reflectance, radiance and brightness temperature products for weather and climate applications. It has sixteen moderate resolution (M-) bands and the Day Night Band (DNB) with 16 detectors at a ground resolution of 750m and five imaging resolution (I-) bands with 32 detectors at a ground resolution of 375m. There are four focal plane assemblies (FPAs) on VIIRS with the Visible Near Infra Red (VNIR) focal plane covering a spectral range of 395-900 nm (bands M1-M7 and I1-I2), the Short and Mid wave Infra Red (SMIR) FPA having a spectral range of 1230-4130 nm (bands M8-M13 and I3-I4), the Long Wave Infra Red (LWIR) FPA with a spectral coverage of 8400-12490 nm (bands M14-M16 and I5) and the single panchromatic high dynamic range Day Night Band (DNB) FPA covering the 500-900 nm spectral region. This paper will focus on the polarization sensitivity of the VNIR FPA where the requirements listed in table 1 apply. The SMIR and LWIR FPAs do not have any polarization sensitivity requirements and their polarization effects were not characterized. Pre-launch characterization of the VIIRS polarization sensitivity was performed for S-NPP, JPSS-1 and JPSS-2 using the same Ground Support Equipment (GSE) and similar testing methodology. This makes comparisons between the sensor's polarization sensitivities easier to interpret since there are no unique GSE effects between tests. The VIIRS radiometric product is contained within the Sensor Data Record (SDR) and is calibrated to an unpolarized scene requirement. Detector-to-detector or HAM side variation in the polarization sensitivity may cause striping in the imagery where the Earth scene is highly polarized. Environmental Data Record (EDR) users, such as the Ocean Color/Chlorophyll (OCC), who use highly polarized scenes in their products, adjust the SDR radiance based on the polarization sensitivity characterization results discussed in this paper. A comparison of the polarization characterization result from JPSS-2 and heritage sensors from S-NPP and JPSS-1 will also be discussing in this paper.

Updated 3/20/14

2. VIIRS POLARIZATION TESTING

2.1 Optical Design Description

The VIIRS optical design's first optical component is the Rotating Telescope Assembly (RTA) that contains an afocal three mirror anastigmat telescope and fold mirror that rotates 360° to view the Earth (scan angles within ±56.03° of nadir) as well as the internal calibration sources. The Half Angle Mirror (HAM) is a fold mirror that rotates at half the speed of the RTA and directs its output energy into the stationary aft optics assembly. The aft optics contain a focusing telescope, two dichroic beam splitters, bandpass filters for spectral selection purposes and the Focal Plane Arrays (FPAs). Each of the VIIRS mirrors has a silver coating with reflectance differences between s and p polarization that are angle of incidence (AOI) dependent. This is important because the HAM's AOI varies between 29.60° to 56.47° during a scan. The means that the HAM's polarization contribution to the sensor's total polarization sensitivity will change depending on the scan angle of the system. The dichroics have intricate and numerous dielectric layers that also produce polarization with strong spectral dependencies. Each band and detector have different AOIs on the dichroics causing the polarization sensitivity from this optical element to vary across detectors within a band. The dielectric layers on the bandpass filters produce polarization effects as well, especially at wavelengths near the edges of the in-band region [5-6].

The mirror coating designs between S-NPP, JPSS-1 and JPSS-2 have remained the same but there are small variations in their performance due to manufacturing tolerances. This led to HAM side differences in the polarization sensitivities for JPSS-1 due to delays between HAM A and B coating runs (S-NPP and JPSS-2 did not have these delays). The dichroic #1 (used for the VNIR bands) thin film design has remained the same as well. However, for band M1, the s and p reflectance is steep and varies between each dichroic build. This causes inconsistency in the polarization sensitivity between sensors for band M1. The bandpass filters have had significant modification between builds [6]. S-NPP VIIRS had optical xtalk and Out-of-Band (OOB) spectral response [7] effects that were corrected on the JPSS-1 VIIRS by modifying the filter design. The unintended consequence is that the bandpass filters produced high levels of polarization sensitivity for bands M1-M4 [5]. The JPSS-2 bandpass filter re-design for band M1-M4 removed the optical xtalk, reduced the OOB spectral response and limited the polarization sensitivity. The results of this improvement in bandpass filter will be discussed section 4.
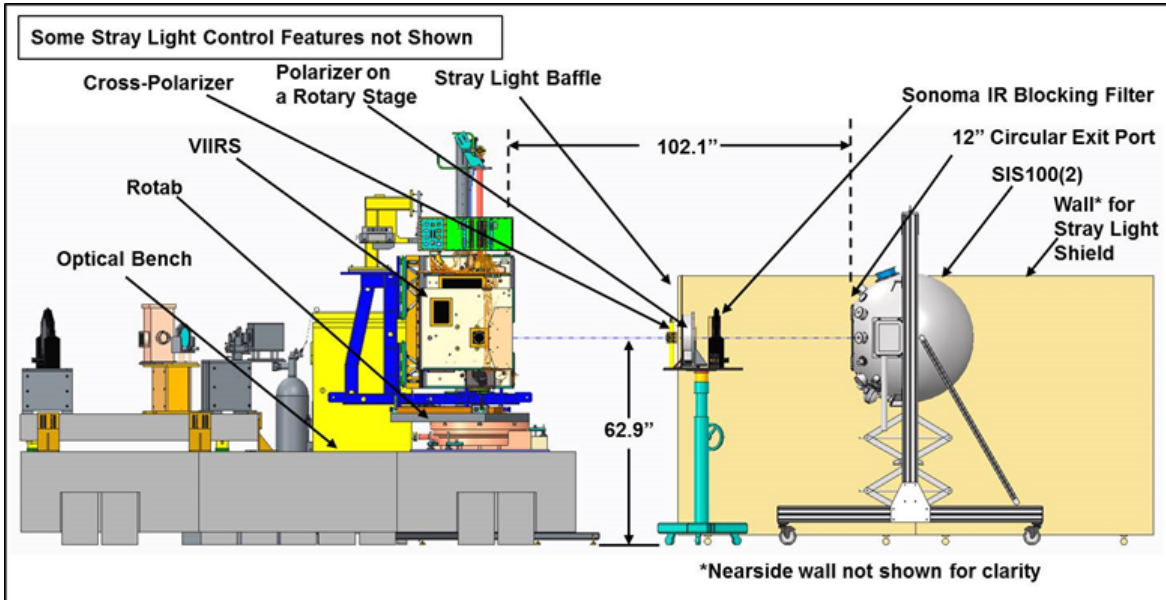

Figure 1:PTSA setup (right side of the figure) with respect to VIIRS (left side of the figure) during the polarization characterization tests

2.2 Polarization Testing

Pre-launch JPSS-2 VIIRS polarization testing data was collected at Raytheon Space and Airborne Systems in El Segundo, California in July of 2016. The Polarization Test Source Assembly (PTSA) was used to characterize the JPSS-2 VIIRS polarization sensitivity. A cartoon of the PTSA and its components are shown in figure 1. It consists of a 100cm diameter Spherical Integration Source (SIS) that provides uniform unpolarized light at several radiance level settings. After the SIS in figure 1 is a full aperture long-wavelength blocking filter (LWBF; i.e., a glass plate with thin film coating that absorbs unwanted light past 625 nm) that is inserted into the optical path only when the blue spectral bands M1 – M3 are tested. This reduces the polarization characterization uncertainties by blocking any OOB leaks in the near infrared spectral region for these bands. Following the LWBF is a polarizing sheet mounted to a rotation stage that can rotate 360° to allow the full two cycle polarization modulation of VIIRS to be measured. The rotation stage is stepped in 15° increments for a total of 25 separate measurements. The polarizing sheet used (BVONIR) is not a perfect polarizer and allows some unpolarized SIS illumination to reach the VIIRS entrance aperture [8]. Next in the optical path is a fixed (i.e., non-rotating) mount to attach a second BVONIR polarizer identical to the one in the rotation stage. VIIRS is used to measure the transmission through the two-sheet combination as a function of rotation stage angle for the first polarizer. When the polarization electric fields of the two sheets are parallel, the transmission through the pair of sheet polarizers is at its maximum. When they are orthogonal, full extinction of the light to VIIRS should occur. This allows the polarization efficiency of the BVONIR sheet to be characterized by rotating on sheet relative to the other fixed sheet. When the polarization orientations are aligned between the two sheets there should be a maximum throughput and when they are orthogonal a minimum output. The amplitude of this modulation (100% for a perfect polarizer) gives the efficiency of the BVONIR polarization sheet. This second BVONIR sheet is only in place for special sheet characterization testing and is removed for the VIIRS polarization sensitivity characterization test runs. The last portion of the PTSA is a baffle system deployed to prevent unwanted light from either the SIS, sheet surface scatter or the surrounding high bay test area from reaching the VIIRS entrance aperture. This prevents unwanted straylight from influencing the characterization results.

Table 1: The VIIRS polarization sensitivity requirements for each band (left table) and the scan angles used to characterize the polarization sensitivity (right table)

Band	Wavelength (nm)	Maximum Amplitude for ±45° Scan Angle	Characterization Uncertainty Requirement in Percent
M1	412	3.0	0.5
M2	445	2.5	0.5
M3	488	2.5	0.5
M4	555	2.5	0.5
M5	672	2.5	0.5
M6	746	2.5	0.5
M7	865	3.0	0.5
I1	640	2.5	0.5
I2	865	3.0	0.5

Scan Angles (degrees)
-55
-45
-37
-30
-20
-15
-8
4
20
45
55

The polarization sensitivity test scans horizontally across the room with a full aperture view of the PTSA for 30 M-band samples and 64 scans with 32 scans each for HAM side. VIIRS uses the internal On-Board Calibrator Blackbody (OBCBB) as a dark reference for background subtraction. These measurements were acquired at 11 unique Earth View scan angles as listed in table 1. Equation 1 shows the offset corrected digital number (dn) which is the sample averaged digital numbers when viewing the PTSA of the Earth View (DN_{EV}) subtracted by the dark digital numbers (DN_{OBCBB}) averaged over the 32 scans of each HAM side. These dns are a function of scan angle θ, polarization angle φ, band b, detector d and HAM side ms.

$$dn(b, d, ms, \theta, \varphi) = \frac{\sum_{scan}\left[\sum_{sample} DN_{EV} - \frac{\sum_{sample} DN_{OBCBB}}{N_{sample\_OBCBB}}\right]}{N_{scan} N_{sample\_EV}} \quad (1)$$

For each band, detector and scan angle measurement, a Fourier filtering using a 2 theta fit with the *dns* as the dependent variable and the polarization angle φ as the independent variable is used as shown in equation 2.

$$dn(b, d, ms, \theta) = \frac{1}{2} a_0 + a_2 \cos 2\varphi + b_2 \sin 2\varphi \quad (2)$$

The average dn signal for that band throughout the 360° polarization angle rotation is captured in the ½ $a0$ dc offset term, the a_2 and b_2 fit the 2φ modulation in the dns from polarization sensitivity effects. Non 2φ frequencies in the dns from detector noise or PTSA artifacts can be used to estimate the uncertainties in the measurement results. The a_0, a_2 and b_2 are then used to compute the polarization amplitude (*PF*) and phase (β), as shown in equations 3 and 4 respectively.

$$PF = \frac{2\sqrt{a_2^2 + b_2^2}}{a_0 F_{cross}} \quad (3)$$

$$\beta = \frac{atan2 \frac{b_2}{a_2}}{2} \quad (4)$$

The F_{cross} term is a scale factor on the amplitude (*PF*) based on the cross-polarization measurements using the two BVONIR sheets. Equation 5 shows how the amplitude of the cross-polarization data is converted to the F_{cross} factor used in equation 3.

$$F_{cross} = \sqrt{\frac{2\sqrt{a_{2\_cross}^2 + b_{2\_cross}^2}}{a_{0\_cross}}} \quad (5)$$

An assumption that both polarization sheets (the fixed and rotation stage ones) have the same efficiencies is made when computing the F_{cross} in equation 5. A *PF* and β for each band, detector, HAM side and scan angle computed and compared to the sensor requirements in table 1. They are plotted in polar plots with the radius term representing the *PF* and polar angle corresponding to twice the β angle (this is due to the 2φ covering 0° to 180° while the polar plot is a full 360° angular extent). These polar plots allow for correlations between bands, detectors, HAM sides and scan angles to be easily visualized. It also helps for comparing results between sensors and investigating root cause (which optical element) in the event of a requirements failure.

3. JPSS-2 VIIRS POLARIZATION RESULTS

Polar plots of the polarization sensitivity for JPSS-2 VIIRS are shown in this section. The x- and y-axis in the polar plots correspond to the a_2 and b_2 terms respectively from equation 2. A vector from the center of the polar plots to each point in the figure can be used to evaluate the polarization amplitude (magnitude of this vector) and phase (half of the angle of the vector with respect to the positive x-axis). Each detector is shown with a connected line of symbols of a common color that is unique to each of the 11 scan angle measurements. Detector 1 (instrument order) has a larger symbol size for sensor coordinate referencing purposes. Visualizing the polarization sensitivity in polar plot fashion allows for amplitude, phase and scan angle variations to be more easily compared since it is in vector form.

Figure 2 shows the polarization sensitivity for bands M1-M4 HAM B for all detectors and each scan angle measured for JPSS-2. The upper left, upper right, lower left and lower right quadrants correspond to bands M1, M2, M3 and M4 respectively. Band M1's polarization amplitude (the radius of the points in figure 2a) is above the 3% requirement in table 1 for all the scan angles in the ±45° requirement range. Bands M2-M4 have less than 2% *PFs* for every detector and scan angle. Bands M1 (figure 2a) and M2 (figure 2b) show large (up to ~1.4%) change in PFs across detectors unlike band M3 (figure 2c) and M4 (figure 2d). This can lead to striping artifacts in the SDR product when viewing scenes with high levels of polarization. At the beginning of scan (-55.5°), the polarization amplitude for band M1 changes by ~1.4% while the phase stays consistent (~2° change) where at the end-of-scan the amplitude is stable (~0.15% change) and the phase has significant change (~10°). This indicates that potential SDR striping due to polarization will likely vary throughout the scan line unlike the Response Versus Scan angle (RVS) and detector-to-detector gain error striping artifacts. Figure 3 shows the JPSS-2 polarization sensitivity polar plots for bands M5 (figure

3a), M6 (figure 3b), M7 (figure 3c), I2 (figure 3d) and I2 (figure 3e) for all HAM side B detectors and scan angles. The polarization amplitude scale for these bands is enlarged in the figure compared to figure 2 so that the small features are easier to observe. These bands pass the polarization sensitivity requirements listed in table 1. Unlike bands M1-M4, these bands have a "wishbone" shape to their polarization sensitivities that changes curvature with scan angle. Since the amplitude the polarization sensitivity for these bands is small, SDR striping should not be a significant issue. The phenomenology causing the "wishbone" pattern across detector and the spread in polarization sensitivity in bands M1-M4 will be discussed in the comparisons section.

4. COMPARISON OF S-NPP, JPSS-1 AND JPSS-2 POLARIZATION SENSITIVIES

A comparison of the S-NPP, JPSS-1 and JPSS-2 HAM A polarization sensitivities as polar plots are shown in figure 4 for bands M1-M4, figure 5 for bands M5-M7 and figure 6 is for bands I1 and I2. Band M1's S-NPP polarization sensitivity (figure 4a) is much lower than JPSS-1 (figure 4a) and JPSS-2 (figure 4b) but has a "wishbone" pattern across its detectors like what was observed in figure 3. The band M1 JPSS-1 polarization has more variation across detector than the other sensors but has a similar spread across the scan angle as the other sensors. Just like JPSS-2, the JPSS-1 polarization sensitivity shows larger phase variation at a scan angle of +55.5° and large amplitude variation at the -55.5° scan angle. The vendor (Raytheon) did extensive modeling of the polarization properties of the VIIRS sensor to understand why this detector behavior exists and what optical elements contribute most to magnitude of the polarization sensitivity [6]. The results of the modeling concluded that the main drivers to the polarization sensitivity of the sensor are from the HAM (contribution changes with scan angle AOI on the mirror), the dichroic beam splitter #1 and the bandpass filters. The HAM contributions can be seen in the variation in the polarization sensitivities over scan angle. This pattern has been consistent between sensor builds with the spread in the detector curves across scan angle remaining roughly constant but the overall magnitude of the polarization sensitivity changing. This makes is due to the HAM mirror coating design remaining the same throughout the JPSS mission. The bandpass filters have changes for each of the sensor builds. As mentioned earlier, the S-NPP bandpasses had optical xtalk and OOB response issues but had low polarization sensitivity. The JPSS-1 bandpass filters were re-worked to remove the optical xtalk effects and reduce the OOB response but have high polarization sensitivities near the edge of their bandpasses. A second re-work of the band M1-M4 bandpass filters for JPSS-2 maintained the optical xtalk and OOB response improvements but also reduce the polarization sensitivity as well. After these updates, expectations were that the polarization sensitivity would be similar to what was observed on S-NPP for JPSS-2. However, the dichroic beam splitter #1 has significant reflectance change in the blue region of the band M1 bandpass. The large slope in reflectance in the band M1 bandpass region has polarization sensitivity that varies significantly between coating runs of dichroics. This causes sensor build-to-build variations in the polarization sensitivity that depends on which dichroic #1 coating run is selected. For S-NPP, the dichroic #1 polarization sensitivity in the band M1 spectral region was low but still was the main contributor to the polarization observed in figures 4-6 for all bands. For JPSS-1, the modeling suggests the dichoric had worse performance than S-NPP in the band M1 spectral region but not as significant as JPSS-2 where the dichroic dominates the sensor level polarization sensitivity. The remaining bands in figure 4: band M2 (figure 4c for S-NPP and JPSS1 and figure 4d for JPSS-2), band M3 (figure 4e for S-NPP and JPSS1 and figure 4f for JPSS-2) and band M4 (figure 4g for S-NPP and JPSS1 and figure 4h for JPSS-2) have similar polarization sensitivities in S-NPP and JPSS-2 where the dichroic beam splitter build-to-build variation is more consistent. Band M5 (figure 5a for S-NPP and JPSS-1 and figure 5b for JPSS-2) has similar polarization sensitivities between JPSS-1 and JPSS-2 due to the new bandpass filters (no changes between these builds) that are not on S-NPP VIIRS. Band M6 (figure 5c for S-NPP and JPSS-1 and figure 5d for JPSS-2) has a similar story where the bandpass filter changes account for the difference between JPSS and S-NPP. Bands M7 (figure 5e for S-NPP and JPSS-1 and figure 5f for JPSS-2) and I2 (figure 6c for S-NPP and JPSS-1 and figure 6d for JPSS-2) have much larger detector-to-detector variation on the JPSS-2 VIIRS than its predecessors. These effects are not well understood (they are within specification so the modeling effort did not cover these bands) as the band M1 build-to-build variations and could be bandpass or dichroic related. The contribution of the polarization sensitivity in the SDR or EDR products for band's M7 and I2 is fairly small and any characterization uncertainties should not degrade them significantly. The last band I1 (figure 6a for S-NPP and JPSS-1 and figure 6b for JPSS-2) shows the JPSS builds to be consistent with the S-NPP being the larger of the VIIRS sensors. Table 2 lists the maximum polarization amplitudes for the three sensor builds with red marking where the requirements were not met. A follow-on paper will discuss in more detail the testing, data processing and measurement uncertainties for the JPSS-2 polarization sensitivity characterization.

5. CONCLUSIONS

The JPSS-2 VIIRS sensor had its polarization sensitivity characterized prelaunch using the same Polarization Test Source Assembly (PTSA) as the S-NPP and JPSS-1 VIIRS sensors. While the S-NPP VIIRS polarization sensitivity met the sensor requirements, the JPSS-1 VIIRS failed for bands M1, M2 and M4 due to large polarization sensitivities in their bandpass filters. Modifications to the JPSS-2 bandpass filter designs for these bands resulted in reduced polarization sensitivities and variations over detectors. However, large polarization sensitivities in the dichroic beam splitter #1 for band M1 on JPSS-2 caused this band to fail the sensor requirement. The remaining JPSS-2 bands are within the sensor requirements and are consistent with the S-NPP or JPSS-1 performance. The lesson learned from the JPSS-2 polarization sensitivity testing is that the dichroic #1 s and p reflectance in the band M1 wavelength region varies significantly between parts. This requires these dichroics to go through part-to-part s and p reflectance testing to understand their actual polarization sensitivity before integration into the sensor. A polarization model that includes measured dichroic, mirror and bandpass filter's s and p reflectances from actual hardware (or high quality witness samples) is needed to make sure these components will allow the sensor level polarization sensitivity to meet its requirements. This characterization of the components and modeling of the sensor level performance is now part of the JPSS-3 and -4 prelaunch testing programs.

Table 2: Each VIIRS sensor's maximum polarization amplitude for each band and scan angle (red indicates a requirements failure)

						Scan Angle						
	Band	-55	-45	-37	-30	-20	-15	-8	4	20	45	55
S-NPP	M1	3.14	2.75	NA	NA	2.02	NA	1.81	NA	1.45	1.22	1.40
	M2	2.26	2.07	NA	NA	1.67	NA	1.54	NA	1.29	1.17	1.30
	M3	1.46	1.33	NA	NA	0.97	NA	0.86	NA	0.62	0.71	0.81
	M4	1.59	1.55	NA	NA	1.37	NA	1.25	NA	1.02	0.88	0.84
	M5	1.19	1.04	NA	NA	0.87	NA	0.85	NA	0.77	0.74	0.70
	M6	1.31	1.17	NA	NA	0.98	NA	0.95	NA	0.89	0.83	0.77
	M7	0.52	0.47	NA	NA	0.42	NA	0.44	NA	0.47	0.47	0.45
	I1	1.52	1.27	NA	NA	0.95	NA	0.86	NA	0.71	0.65	0.62
	I2	0.28	0.28	NA	NA	0.30	NA	0.33	NA	0.37	0.36	0.34
JPSS-1	M1	5.56	5.74	5.87	6.02	6.17	6.21	6.32	6.43	6.41	6.17	5.95
	M2	4.07	4.10	4.12	4.22	4.18	4.20	4.22	4.26	4.19	4.36	4.47
	M3	2.92	2.87	2.83	2.85	2.76	2.75	2.74	2.74	2.85	3.08	3.12
	M4	4.03	4.21	4.33	4.35	4.32	4.36	4.30	4.29	4.15	3.99	3.91
	M5	2.10	2.17	2.22	2.19	2.13	2.14	2.07	2.04	2.02	1.99	1.98
	M6	1.62	1.32	1.13	1.00	0.87	0.92	0.91	0.95	0.96	0.95	0.95
	M7	1.19	0.92	0.74	0.61	0.48	0.47	0.43	0.46	0.47	0.55	0.60
	I1	0.85	0.90	0.95	0.95	0.94	1.00	0.95	0.99	1.00	1.03	1.04
	I2	1.19	0.92	0.75	0.63	0.50	0.51	0.48	0.50	0.52	0.61	0.66
JPSS-2	M1	4.22	4.25	4.32	4.42	4.59	4.64	4.73	4.82	4.85	4.72	4.53
	M2	1.73	1.52	1.44	1.38	1.31	1.33	1.30	1.33	1.50	1.70	1.77
	M3	1.14	1.01	0.97	0.93	0.88	0.90	0.91	1.03	1.14	1.27	1.33
	M4	0.89	0.94	0.95	1.03	1.08	1.12	1.13	1.15	1.15	1.12	1.07
	M5	1.60	1.60	1.58	1.60	1.57	1.58	1.53	1.52	1.54	1.52	1.49
	M6	1.49	1.24	1.08	0.99	0.91	0.88	0.85	0.85	0.85	0.86	0.86
	M7	1.08	0.96	0.88	0.85	0.90	0.94	0.98	1.05	1.13	1.21	1.25
	I1	0.81	0.80	0.81	0.84	0.84	0.86	0.86	0.86	0.87	0.88	0.87
	I2	1.14	1.03	0.97	1.02	1.10	1.14	1.19	1.27	1.35	1.43	1.46

REFERENCES

[1] Welsch, C., Swenson, H., Cota, S. A., DeLuccia, F., Haas, J. M., Schueler, C., Durham, R. M., Clement, J. E., and Ardanuy, P. E., "VIIRS (Visible Infrared Imager Radiometer Suite): A Next-Generation Operational Environmental Sensor for NPOESS," Intl. Geoscience and Remote Sensing Symposium (IGARSS) Proceedings, (2001).

[2] Kramer, H.J., "Observation of the Earth and Its Environment: Survey of Missions and Sensors," 4th Edition, Springer-Verlag, ISBN: 3540423885, May (2002).

[3] Salomonson, V., Barnes, W., Xiong, X., Kempler, S., and Masuoka, E., "An Overview of the Earth Observing System MODIS Instrument and Associated Data Systems Performance," Intl. Geoscience and Remote Sensing Symposium (IGARSS) Proceedings (2002).

[4] Holben, B. N., Kaufman, Y. J., and Kendall, J. D., "NOAA-11 AVHRR visible and near-IR inflight calibration," Int. J. Remote Sensing, vol. 11, pp.1511 -1519 1990

[5] McIntire, J., Young, J., Moyer, D, Waluschka, E., Oudrari, H., and Xiong, X., "Analysis of JPSS J1 VIIRS Polarization Sensitivity Using the NIST T-SIRCUS," Proceedings of SPIE Vol. 9607 (2015).

[6] Waluschka, E., McCorkel, J., McIntire, J., Moyer, D., McAndrew, B., Brown, S., Lykke, K., Young, J., Fest, E., Butler, J., Wang, T., Monroy, E., Turpie, K., Meister, G. and Thome, K., "VIIRS/J1 Polarization Narrative," Proceedings of SPIE Vol. 9607 (2015).

[7] Feeley, J., Moyer, D., and De Luccia, F., "SNPP VIIRS Spectral Response Lessons Learned and Their Impacts on JPSS VIIRS Performance," Intl. Geoscience and Remote Sensing Symposium (IGARSS) Proceedings, (2005).

[8] Moyer, D., McIntire, J., Young, J., McCarthy, J., Waluschka, E., Xiong, X., and De Luccia, F., "JPSS-1 VIIRS Pre-launch Polarization Testing and Performance," IEEE TGRS, 99-113 (14 January 2017).
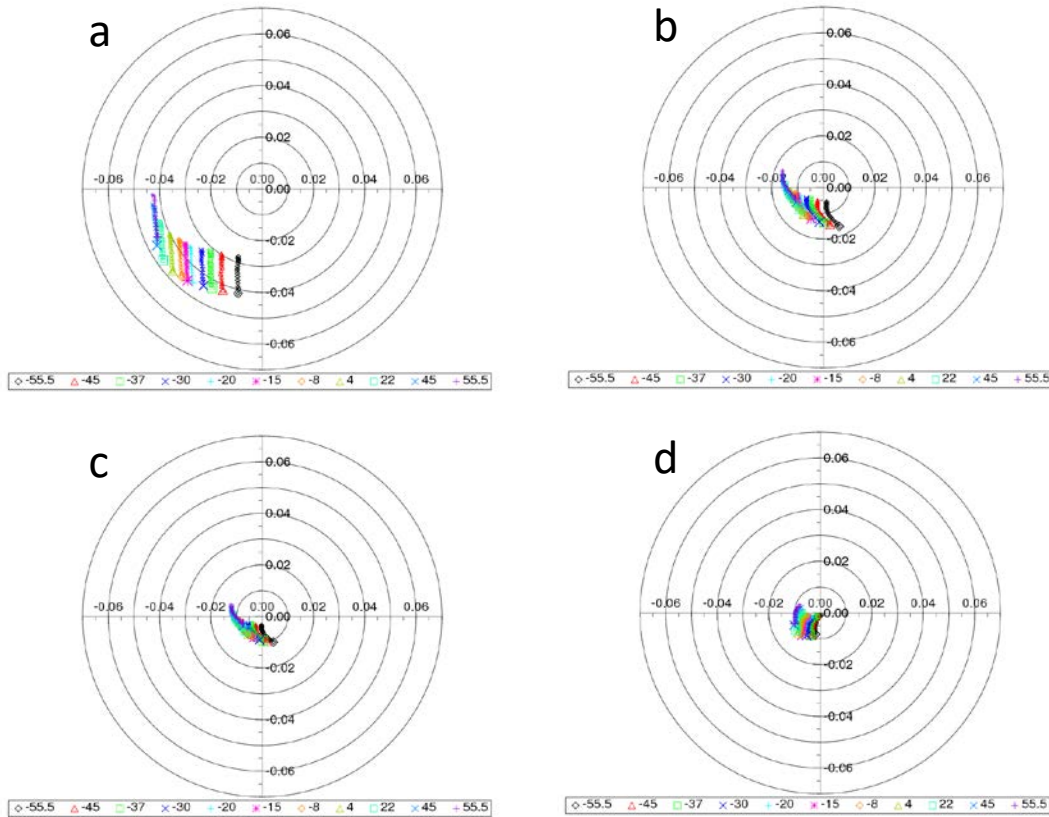
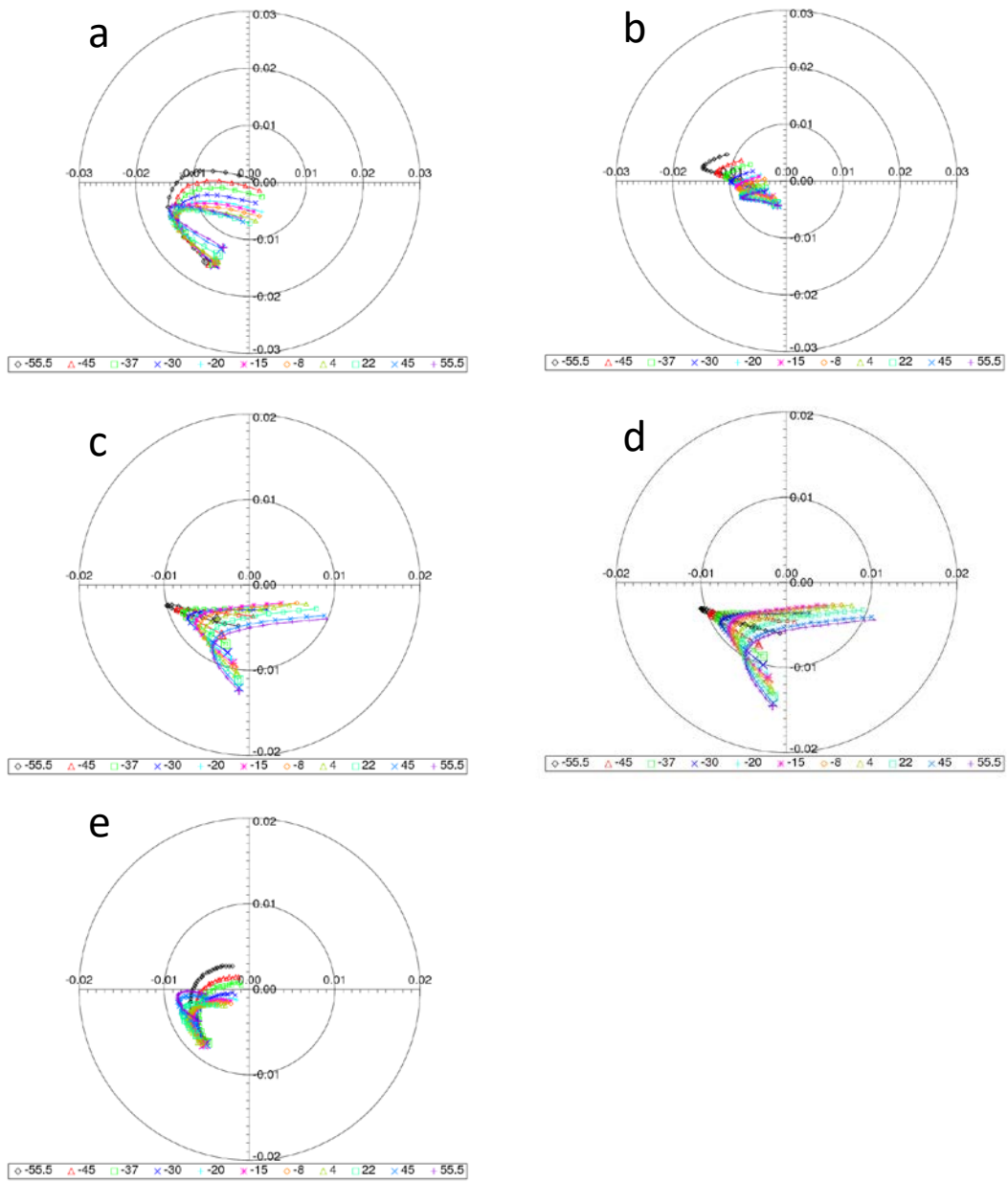**Figure 2: Polar plots of the JPSS-2 VIIRS HAM B polarization sensitivity for bands M1 (a), M2 (b), M3(c) and M4(d)**

Figure 3:Polar plots of the JPSS-2 VIIRS HAM B polarization sensitivity for bands M5 (a), M6 (b), M7 (c), I2(d) and I1(e)
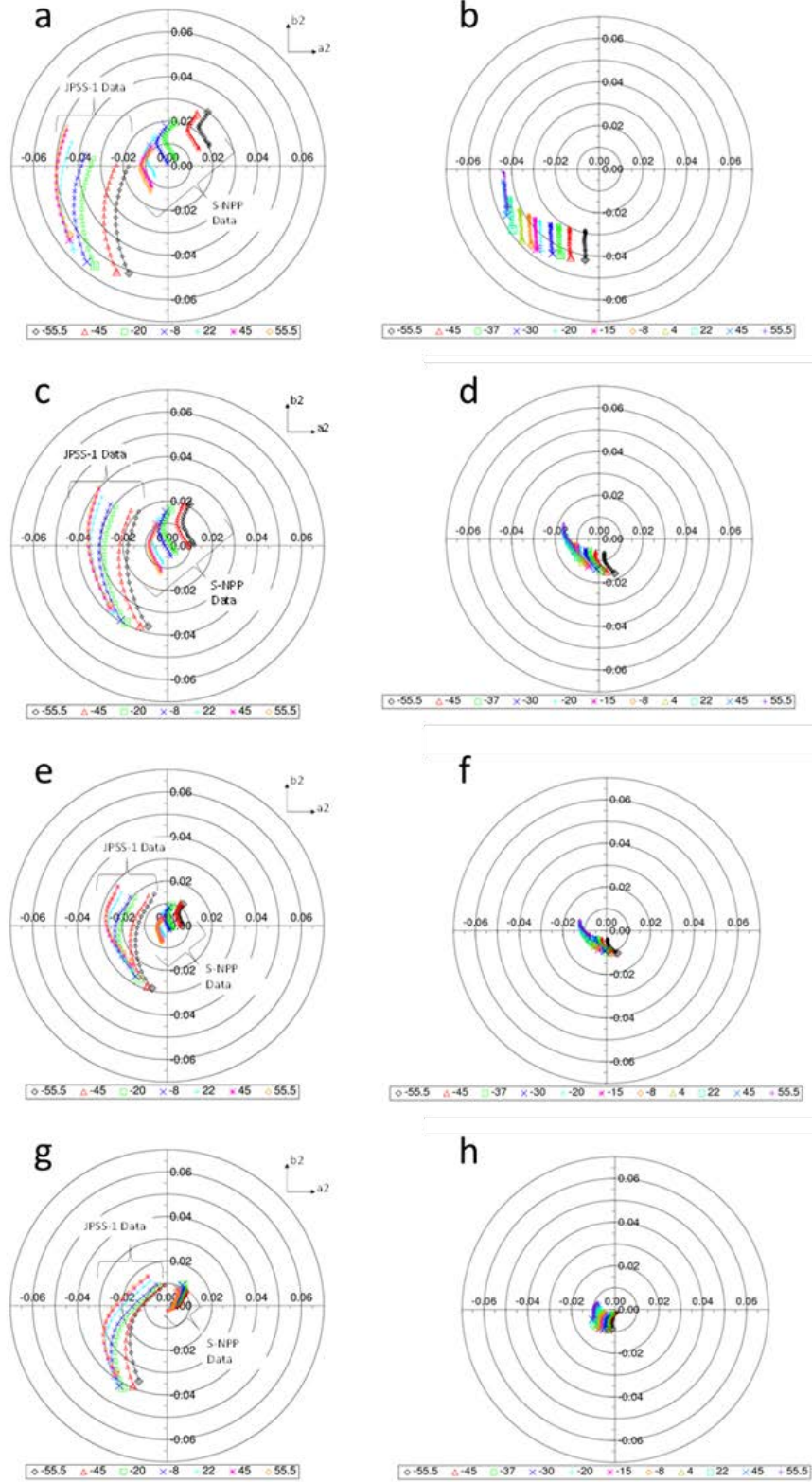
Figure 4: Polar plots of S-NPP and JPSS-1 VIIRS (left column) and JPSS-2 (right column) HAM A polarization sensitivity for bands M1 (a and b), M2 (c and d), M3 (e and f) and M4 (g and h)
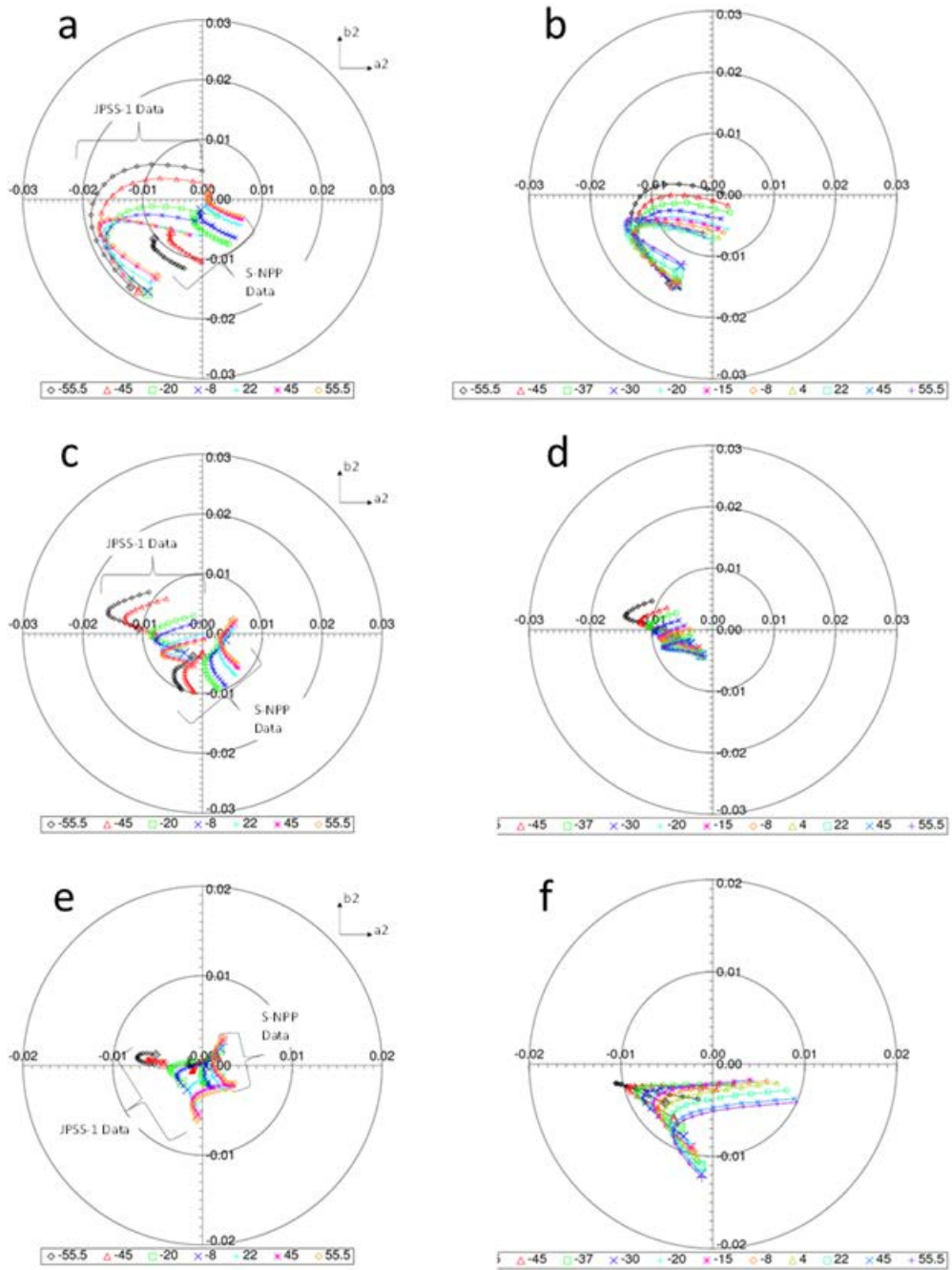
Figure 5: Polar plots of S-NPP and JPSS-1 VIIRS (left column) and JPSS-2 (right column) HAM A polarization sensitivity for bands M5 (a and b), M6 (c and d) and M7 (e and f)
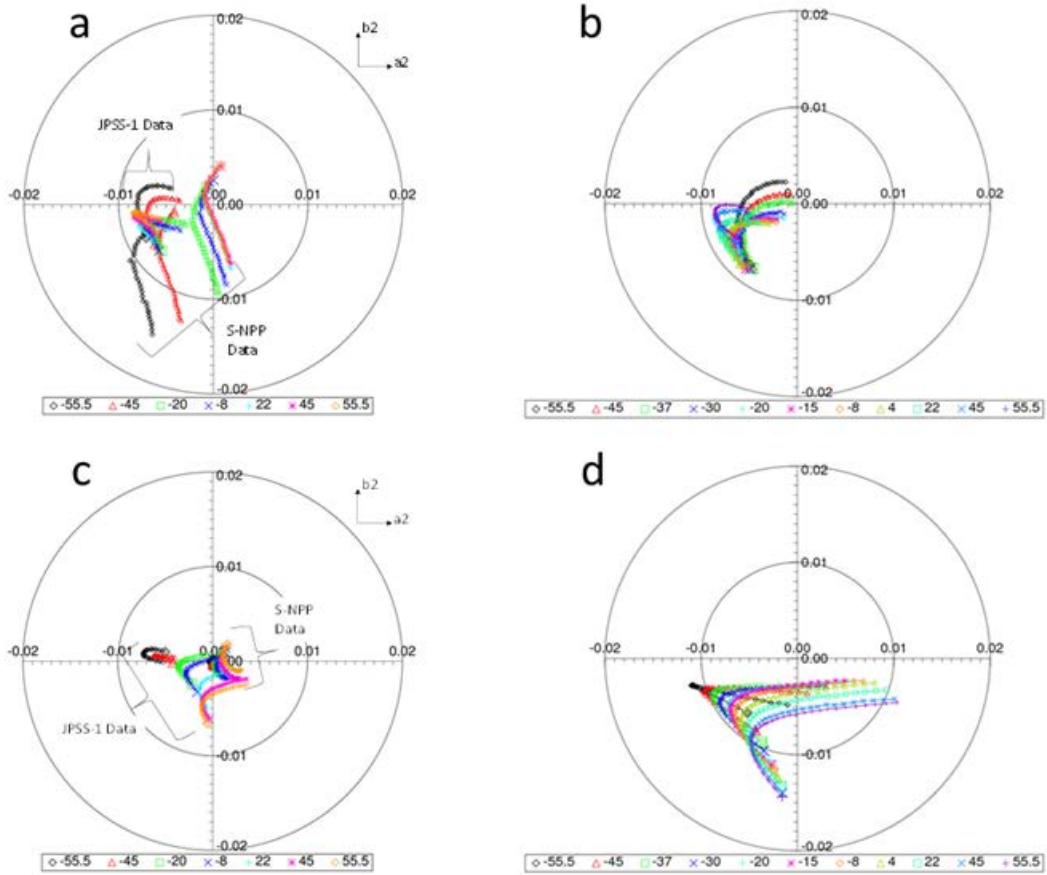
Figure 6: Polar plots of S-NPP and JPSS-1 VIIRS (left column) and JPSS-2 (right column) HAM A polarization sensitivity for bands I1 (a and b) and I2 (c and d)